



# Status of Interatomic Potentials Models for Hydrogen Energy Applications

SAND2018-2004C  
 



## European Advanced Energy Materials and Technology Congress Stockholm, Sweden, March 25-28, 2018

X. W. Zhou, R. B. Sills, M. E. Foster, R. A. Karnesky, M. D. Allendorf, V. Stavila

<sup>1</sup>Sandia National Laboratories, USA

T. W. Heo, B. C. Wood, S. Kang

<sup>2</sup>Lawrence Livermore National Laboratory, Livermore, California 94550, USA

Sandia National Laboratories is a multi-mission laboratory managed and operated by National Technology and Engineering Solutions of Sandia, LLC., a wholly owned subsidiary of Honeywell International, Inc., for the U.S. Department of Energy's National Nuclear Security Administration under contract DE-NA-0003525. Lawrence Livermore National Laboratory is operated for the US Department of Energy under Contract DE-AC52-07NA27344. The authors gratefully acknowledge research support from the U.S. Department of Energy, Office of Energy Efficiency and Renewable Energy, Fuel Cell Technologies Office, under Contract Numbers DE-AC04-94AL85000 and DE-AC52-07NA27344.

# Outline

1. Embedded-atom method potential for Fe-Ni-Cr-H
2. Analytical bond order potential for Al-Cu-H
3. Analytical bond order potential for Mg-H

# Four criteria of fidelity of Fe-Ni-Cr interatomic potential

1. permit stable high temperature MD simulations
2. capture the correct stacking fault energy ( $\gamma_{sf}$ )
3. prescribe well the elastic constants
4. give reasonable energy and volume for various compositions

# Issues of literature potentials

1. The potential we published (CALPHAD 1993, 17, 383) did not consider the four criteria
2. Smith and Was' potential (PRB 1989, 40, 10322) was fitted to effective atoms and did not consider stacking fault energy
3. The 2013 version of Bonny et al's potential (MSMSE 2013, 21 085004) incorrectly predicts phase separation



4. The 2011 version of Bonny et al's potential (MSMSE 2011, 19, 085008) incorrectly predicts negative slope of stacking fault energy with Ni composition
5. Tong et al's potential (Mol. Sim. 2016, 42, 1256) incorrectly predicts large negative stacking fault energy ( $\sim -200 \text{ mJ/m}^2$ )

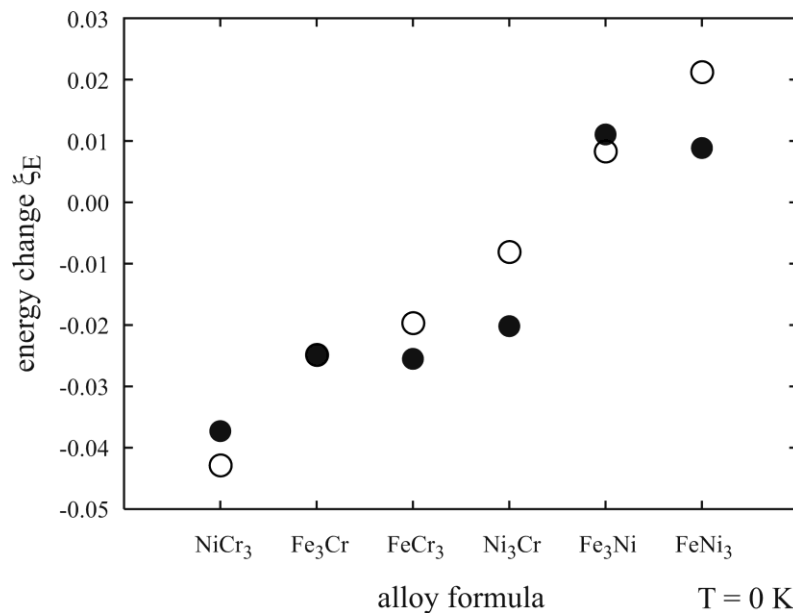


# Current status of our Fe-Ni-Cr-H embedded-atom method potential

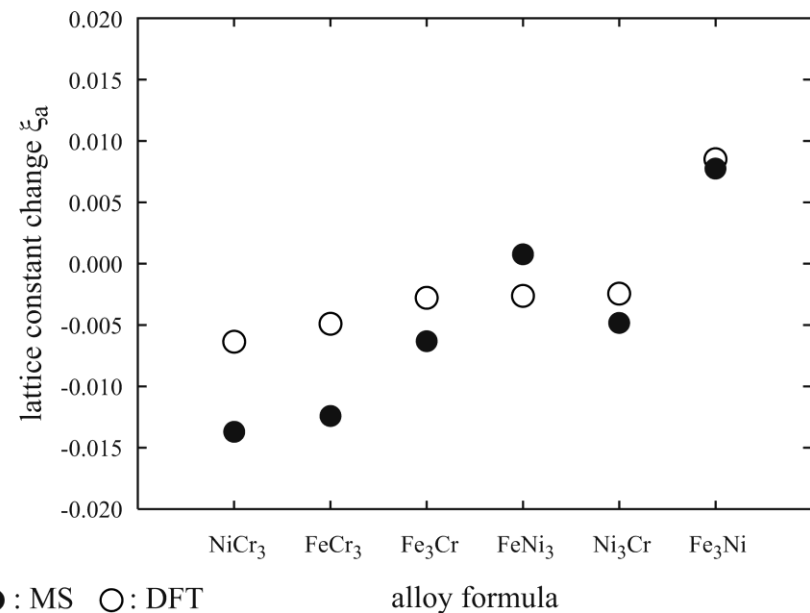
.....

# Energy and volume trends

(a) Energy



(b) Lattice constant



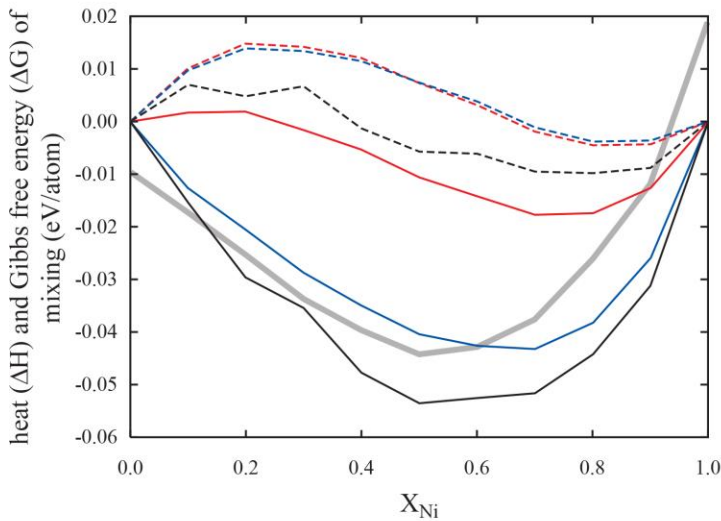
## Swelling parameter comparison with experiments

solute	fcc Fe		bcc Fe		
	MS	DFT	MS	DFT	exp.
Ni	3.46%		10.09%		4.65%
Cr	-20.82%		8.06%		4.36%

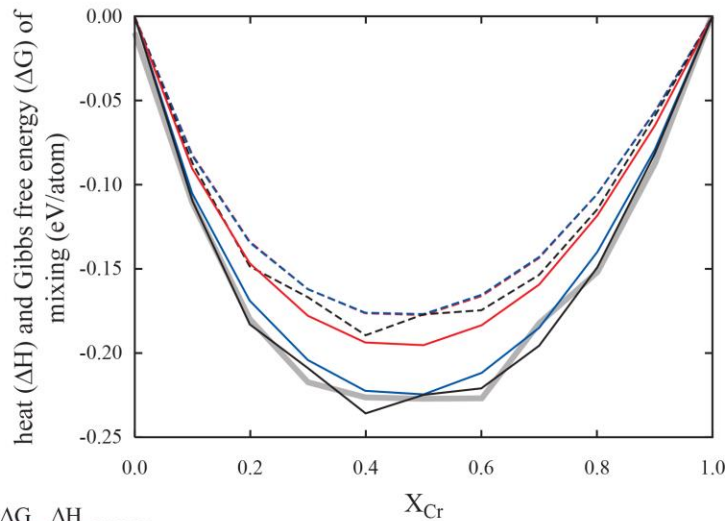
Experimental data from King, J. Mater. Sci. 1966, 1, 79

# Heats and Gibbs free energy of solution

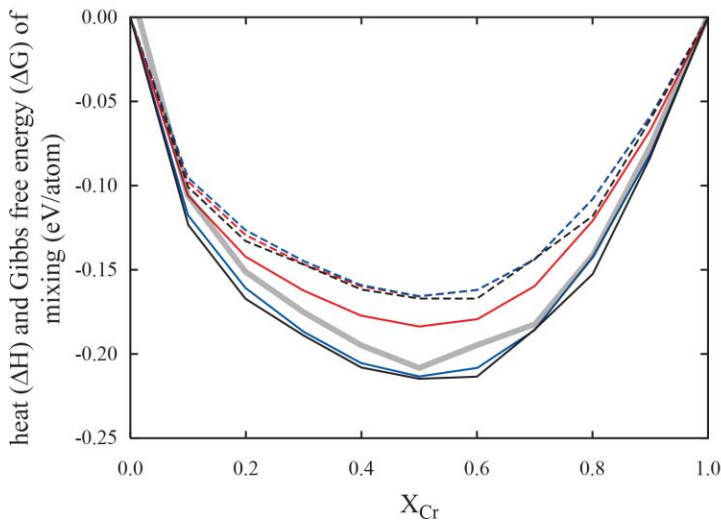
**(a)** Fe-Ni



**(b)** Fe-Cr

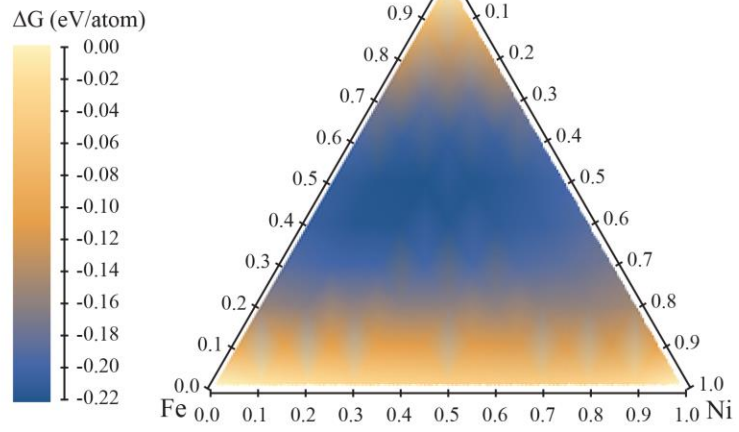


**(c)** Ni-Cr



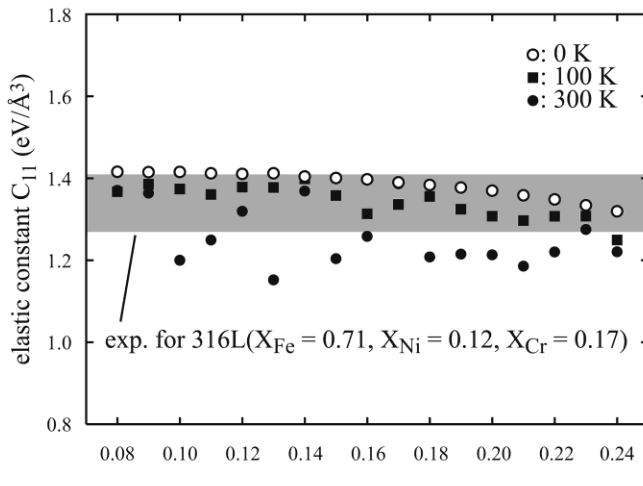
$\Delta G$     $\Delta H$   
 ——— 300 K  
 - - - 800 K  
 ——— 800 K, +2% V  
 ——— 800 K, +2% V, bcc

**(d)**  $\Delta G$  of Fe-Ni-Cr (0% V) at 800 K

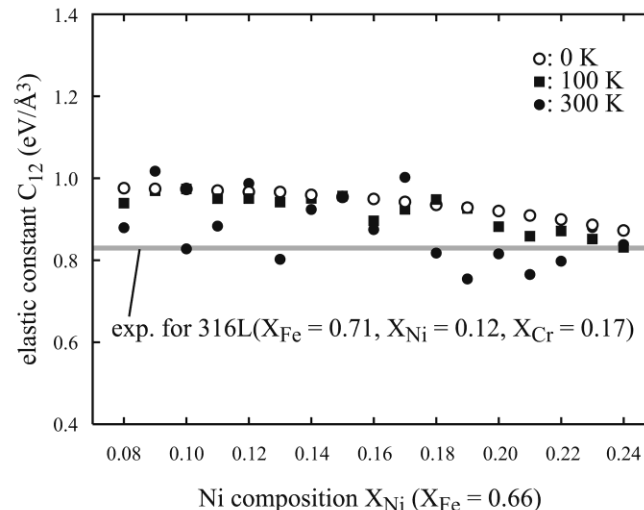


# Elastic constants

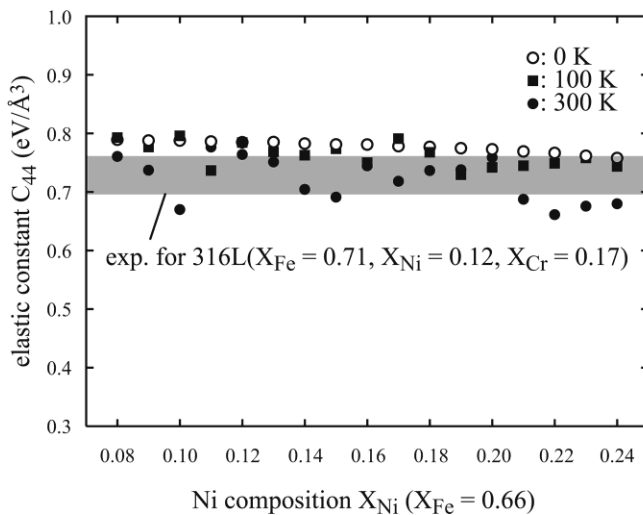
(a)  $C_{11}$



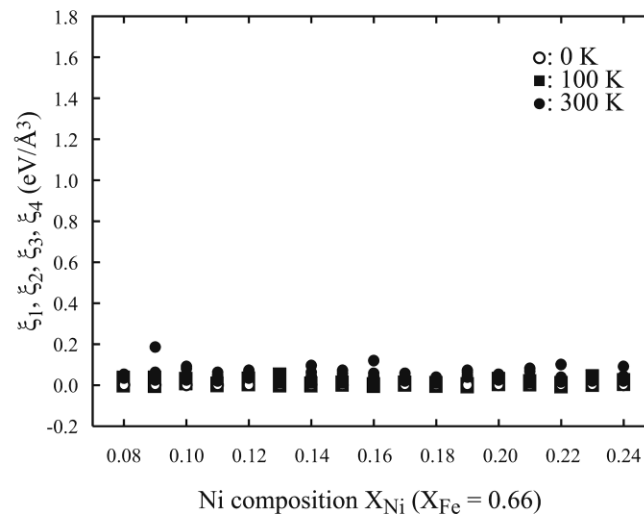
(b)  $C_{12}$



(c)  $C_{44}$



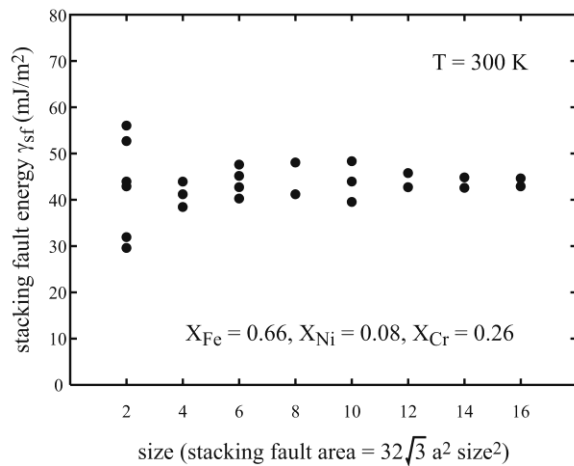
(d)  $\xi_1, \xi_2, \xi_3, \xi_4$



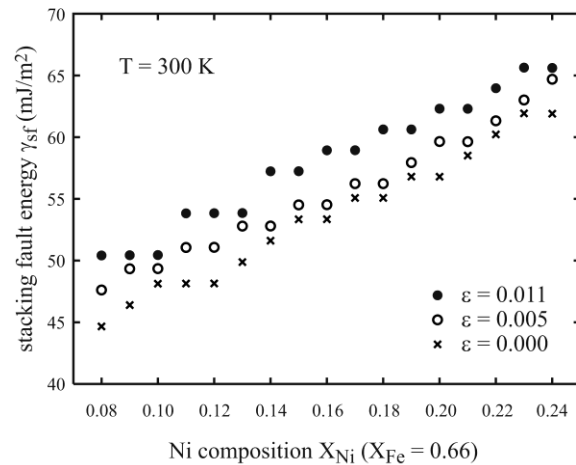
Experimental data for 316L from Ledbetter, Ultrasonics 1985, 23, 9; Bonny et al, MSMSE 2011, 19, 085008; Bonny et al, MSMSE 2013, 21, 085004.

# Stacking fault energy

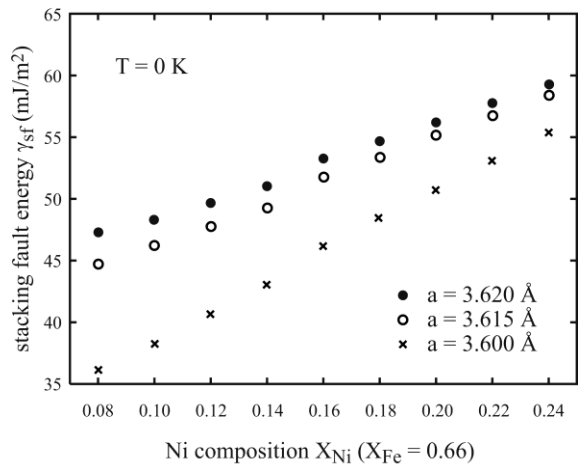
(a) Convergence of MD stacking fault energy



(b) Converged MD stacking fault energy vs.  $X_{Ni}$



(c) DFT (EMTO-CPA) stacking fault energy vs.  $X_{Ni}$

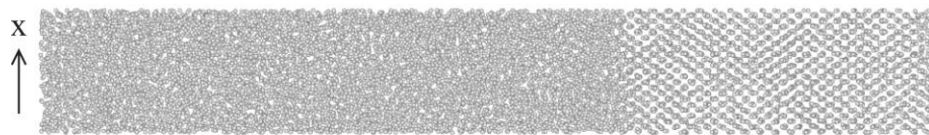


The predicted stacking fault energies match well with experimental results (see, for example, Vitos et al, PRL 2006, 96, 117210, and references therein).

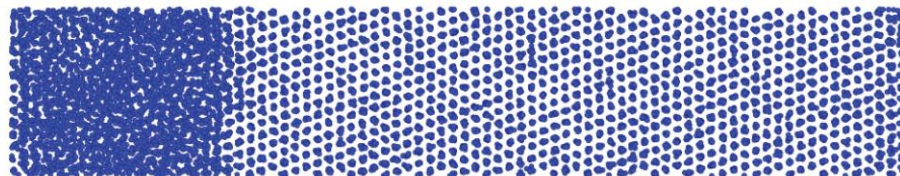


# Melting

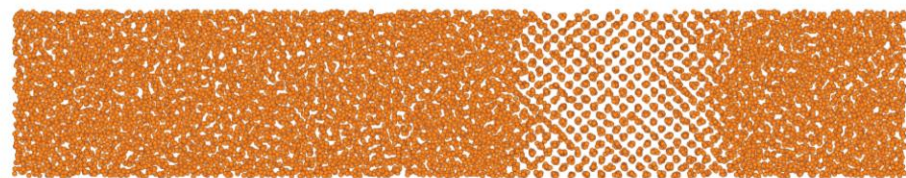
**(a)** bcc Fe



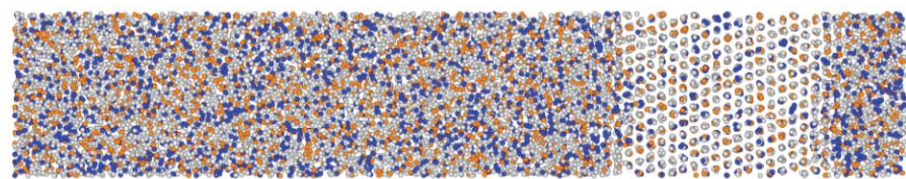
**(b)** fcc Ni



**(c)** bcc Cr

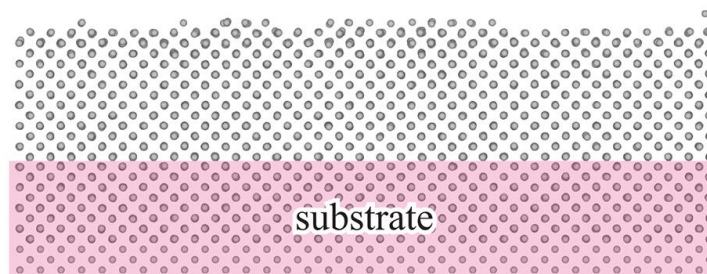


**(d)** fcc  $Fe_{0.6}Ni_{0.2}Cr_{0.2}$

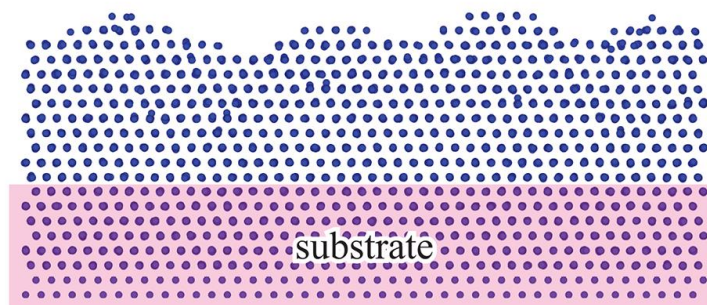


# Growth simulations

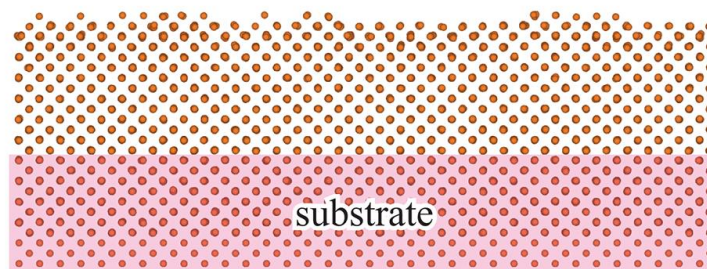
(a) Fe on bcc Fe, atom map



(b) Ni on fcc Ni, atom map



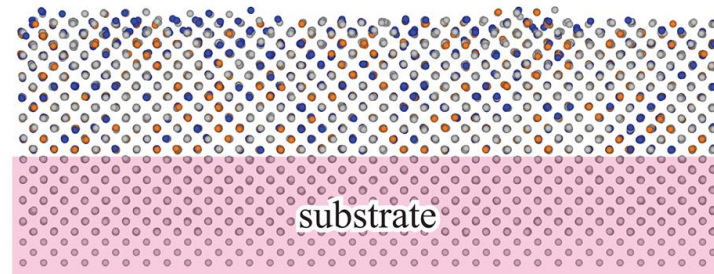
(c) Cr on bcc Cr, atom map



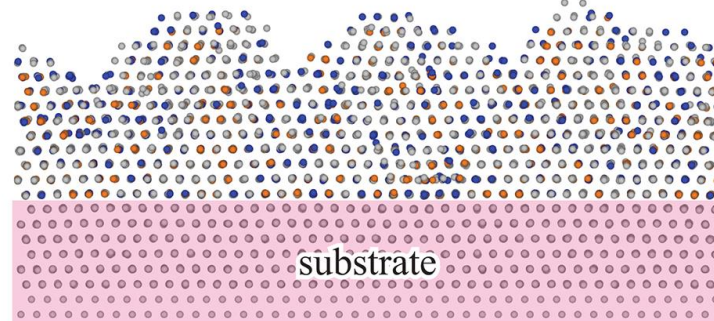
atom: ● Fe ● Cr ● Ni

structure: ● fcc ● bcc ● hcp ● undefined

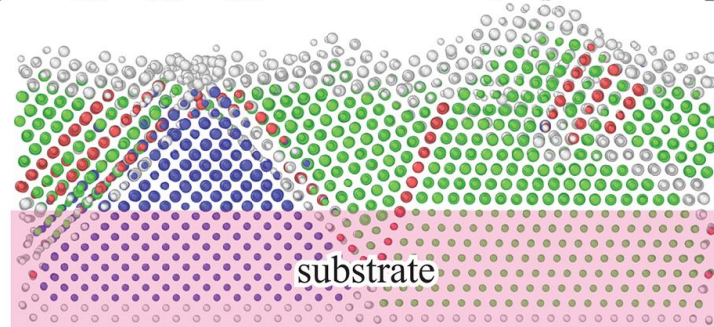
(d)  $\text{Fe}_{0.6}\text{Ni}_{0.2}\text{Cr}_{0.2}$  on bcc Fe, atom map



(e)  $\text{Fe}_{0.6}\text{Ni}_{0.2}\text{Cr}_{0.2}$  on fcc Fe, atom map



(f)  $\text{Fe}_{0.6}\text{Ni}_{0.2}\text{Cr}_{0.2}$  on fcc+bcc Fe, structure map



bcc: x [100], y [010], z: [001] fcc: x [112], y [111], z [110] 1 nm

$T = 300 \text{ K}$ ,  $E_i = 0.1 \text{ eV}$ ,  $R \sim 0.5 \text{ nm/ns}$

# Current status of our Al-Cu-H analytical bond order potential

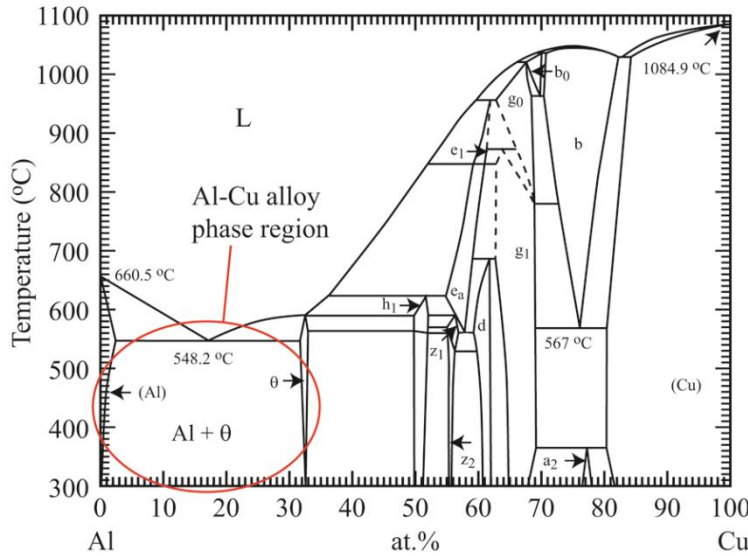
.....

1. X. W. Zhou, D. K. Ward, and M. E. Foster, *J. Alloys Compds.* 2016, 680, 752;
2. X. W. Zhou, D. K. Ward, M. Foster, J. A. Zimmerman, *J. Mater. Sci.*, 2015, 50, 2859.

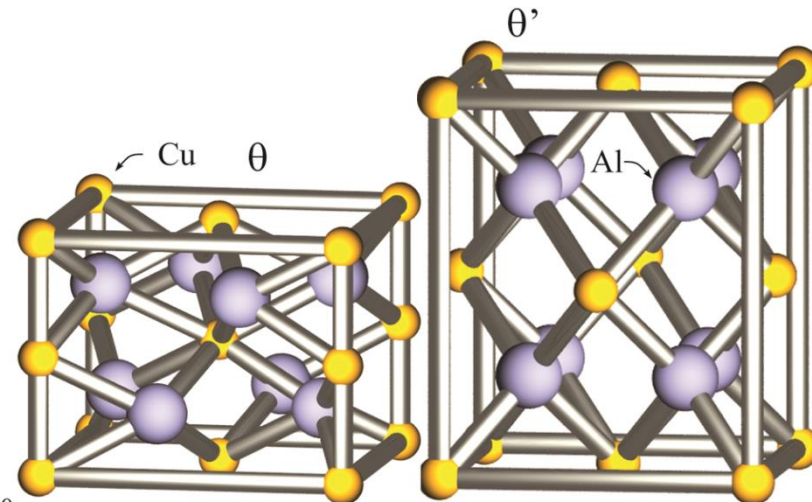
# Wish list for Al-Cu-H potential

1. A high stacking fault energy of Al observed in experiments;
2. Properties trends of a variety of stable and metastable structures;
3. Al-rich side of the Al-Cu phase diagram;
4. A reasonable positive heat of solution of Cu in Al;
5.  $H_2 \rightleftharpoons 2H$  chemical reaction;
6.  $Al_{1-x}H_x \rightarrow Al + H_2$  and  $Cu_{1-x}H_x \rightarrow Cu + H_2$  phase separations;
7. Robust MD simulations.

**(a)** Al-Cu phase diagram



**(b)** crystal structure of the  $\theta$  and  $\theta'$  phases



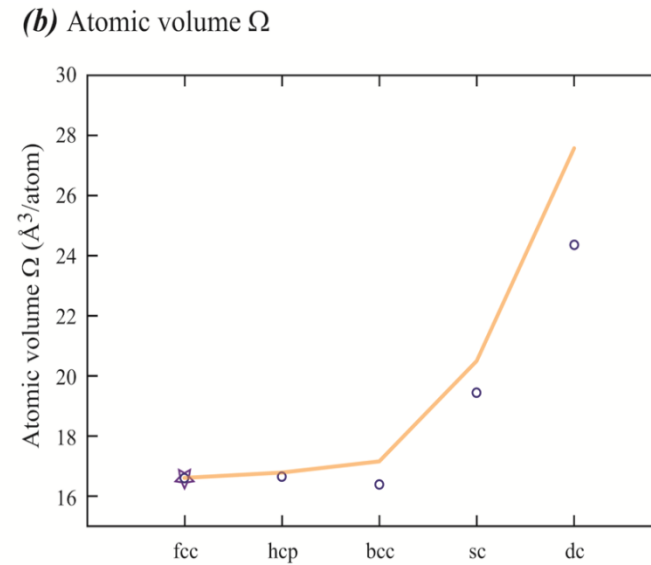
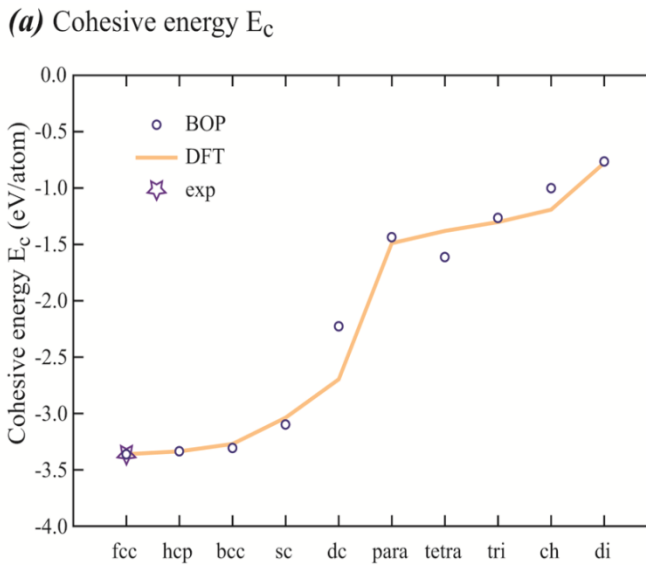
# Stacking fault energy of Al

Model/Exp.	$\gamma_{100}$	$\gamma_{110}$	$\gamma_{111}$	$\gamma_{sf}$
EAM-CY	583	631	526	1
EAM-Mishin1	947	1013	873	141
EAM-BAM	1017	1154	1003	85
EAM-VC	862	969	829	71
EAM-MSAH	194	328	138	126
EAM-Zhou	868	958	832	44
EAM-MKBA	495	582	427	125
EAM-JNP	977	1055	910	0
MEAM	903	944	599	141
REAX-LJGS	481	483	427	0
REAX- Ojwang	810	848	711	1
BOP	979	1069	850	133
DFT [38]	1063	1098	987	-----
Exp. [59,60,61,62]	980-1140	980-1140	980-1140	120-144

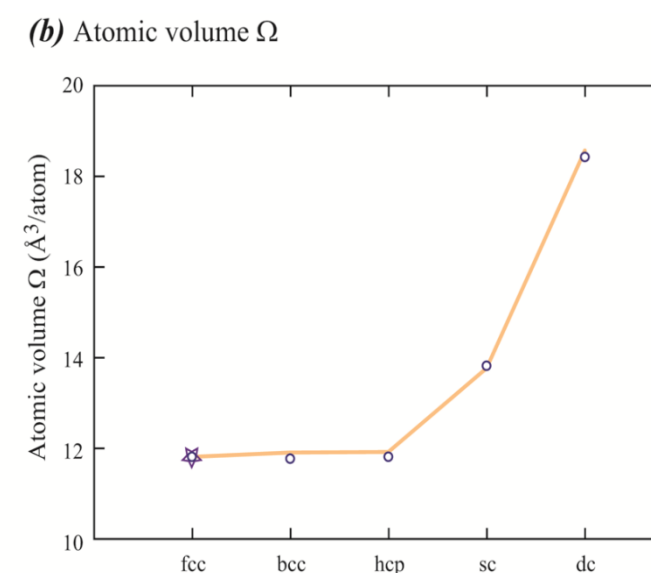
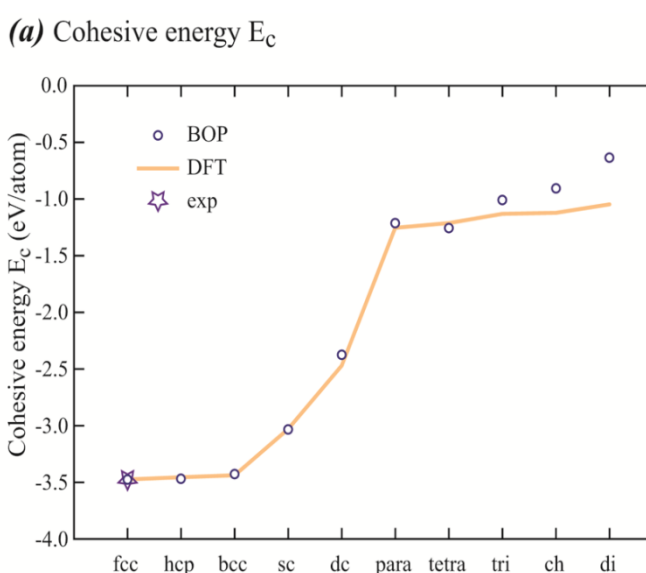
BOP captures a high stacking fault energy of Al.

# Property trends of Al and Cu

Al



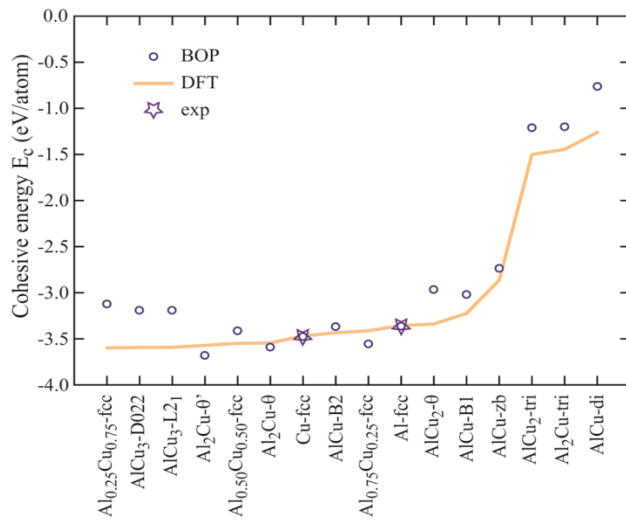
Cu



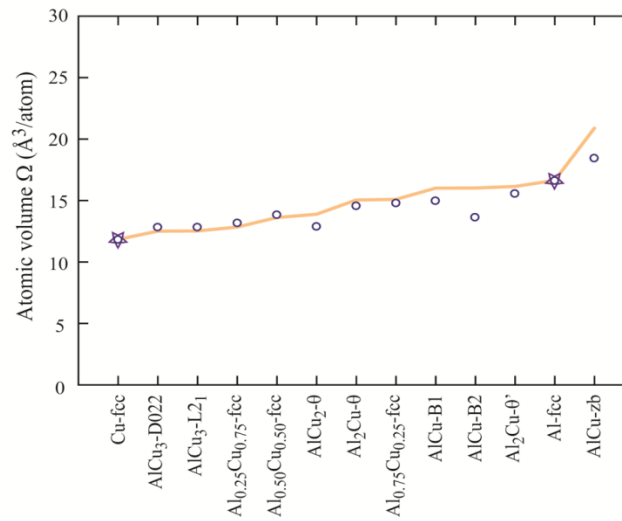
Pretty good property trends for Al and Cu.

# Property trends of Al-Cu

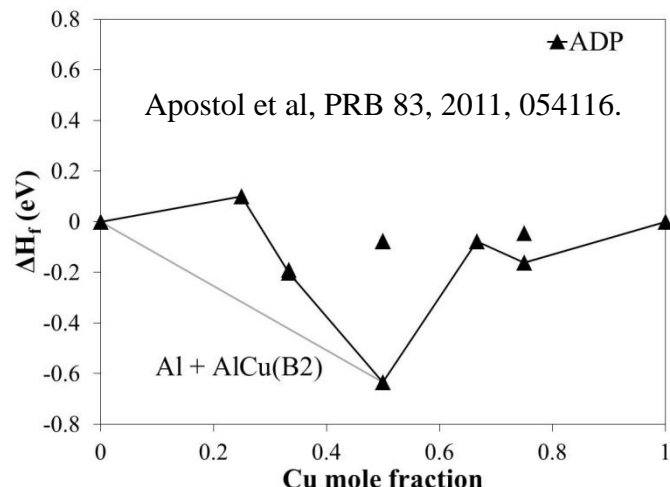
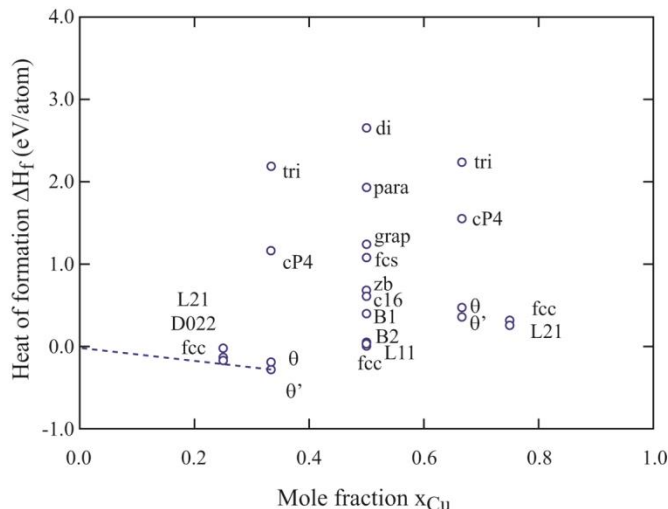
(a) Cohesive energy  $E_c$



(b) Atomic volume  $\Omega$



## Heat of formation vs. composition



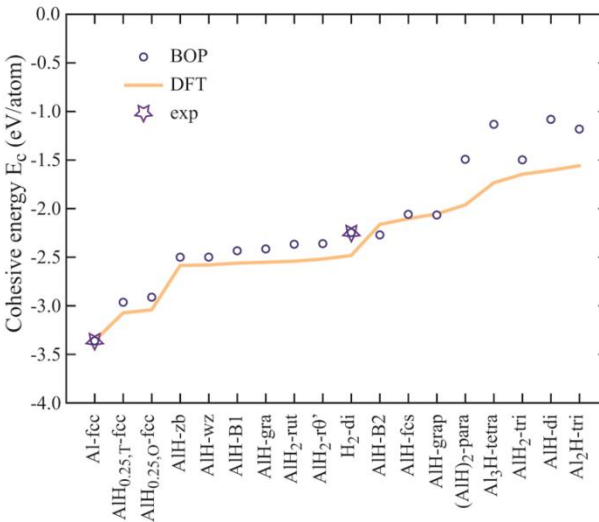
Pretty good property trends for AlCu.

# Property trends of Al-H and Cu-H

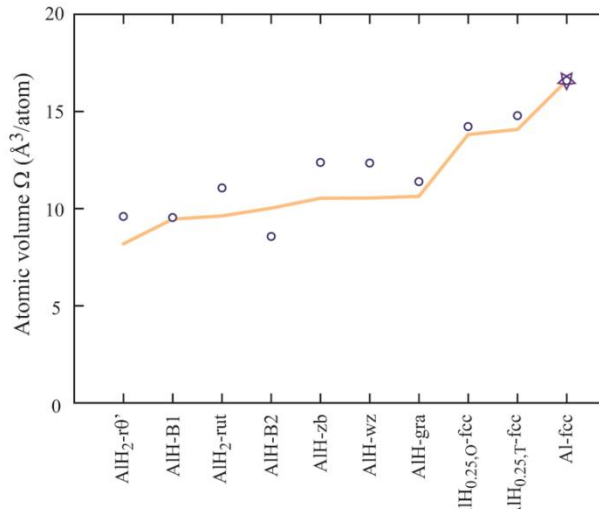
**AlH**

**(a)**

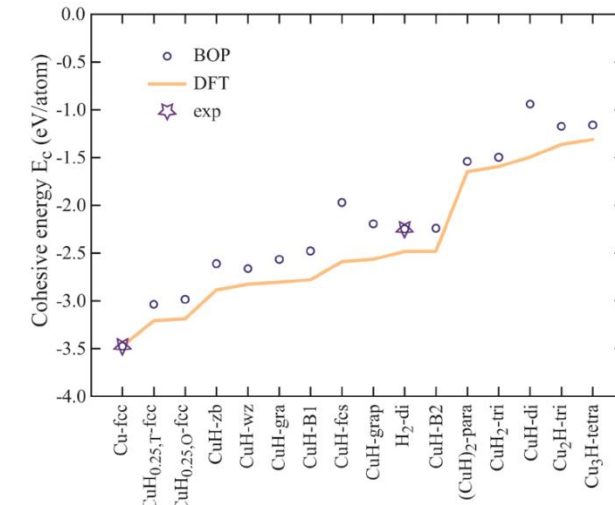
Cohesive energy  $E_c$



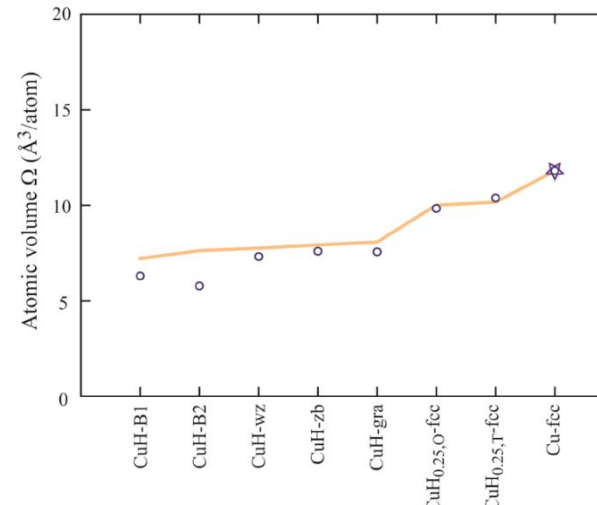
**(b)** Atomic volume  $\Omega$



**(a)** Cohesive energy  $E_c$



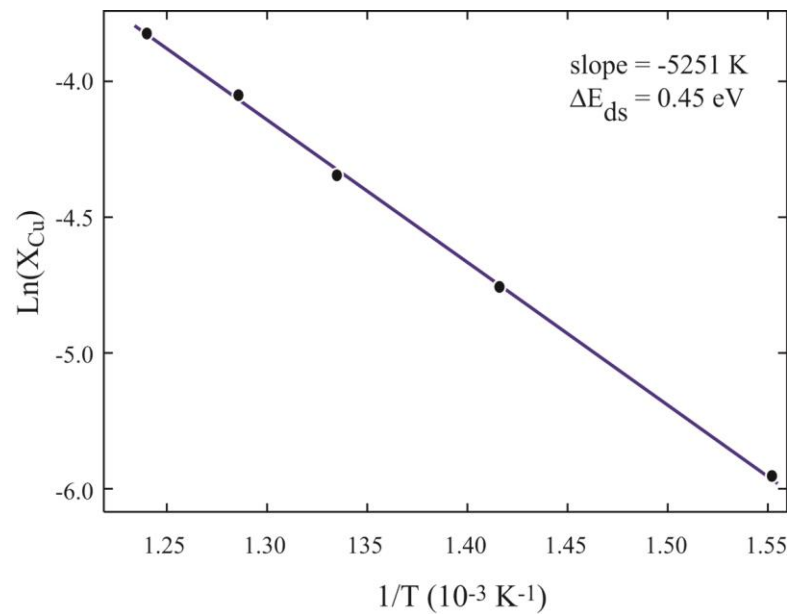
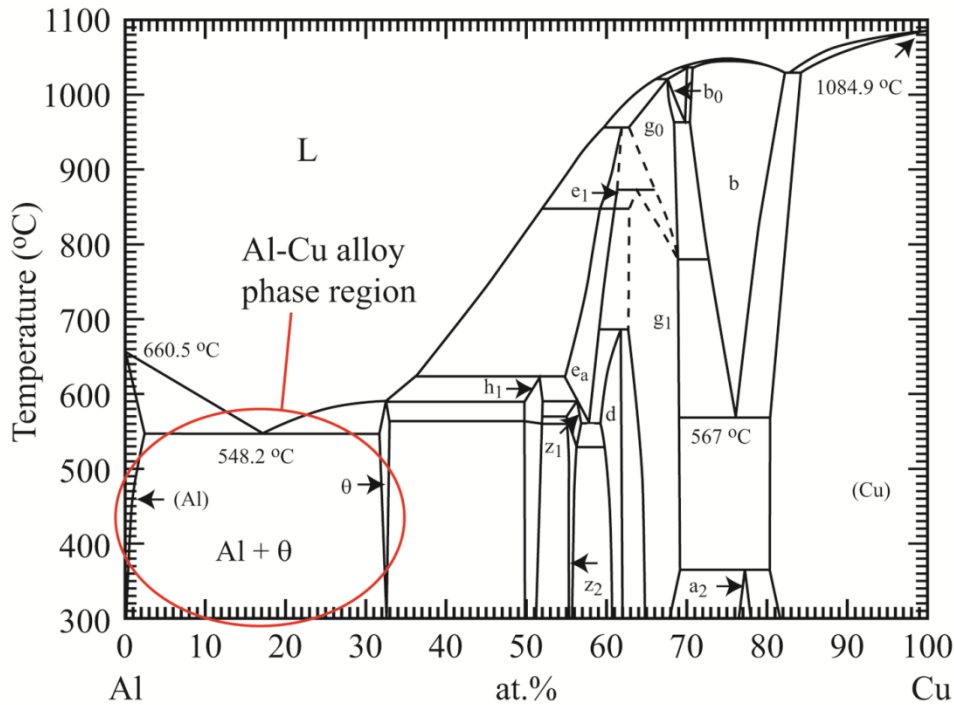
**(b)** Atomic volume  $\Omega$



**CuH**

Pretty good property trends for AlH and CuH.

# Dilute heat of solution of Cu in Al



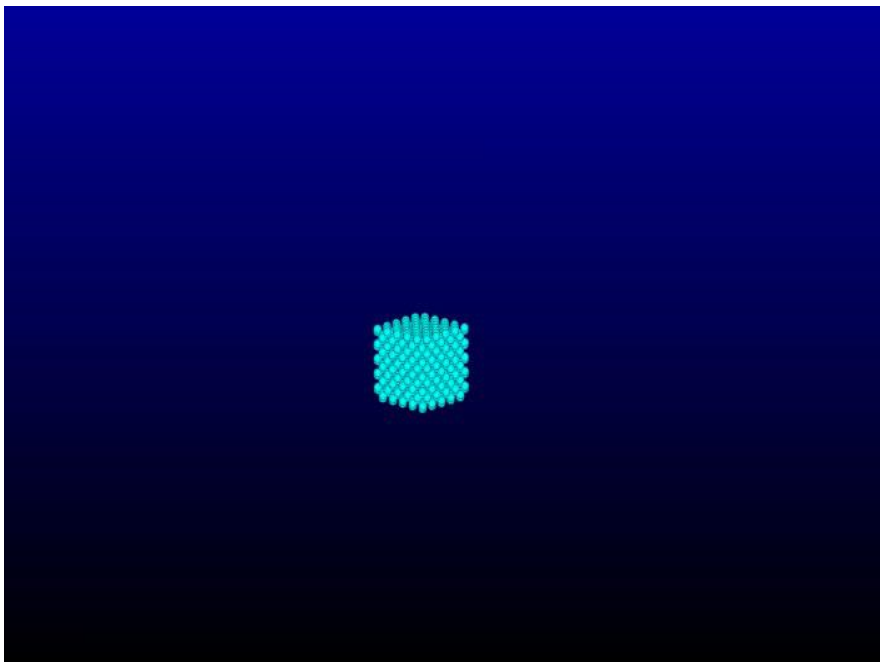
1. Traditionally, heat of solution of Cu in Al is taken as energy change due to taking a Cu atom from Cu pool and putting it in Al pool;
2. Should really be the energy change due to taking a Cu atom from  $\text{Al}_2\text{Cu}$  pool and putting it in Al pool;
3. Must be a positive number

## Literature comparison

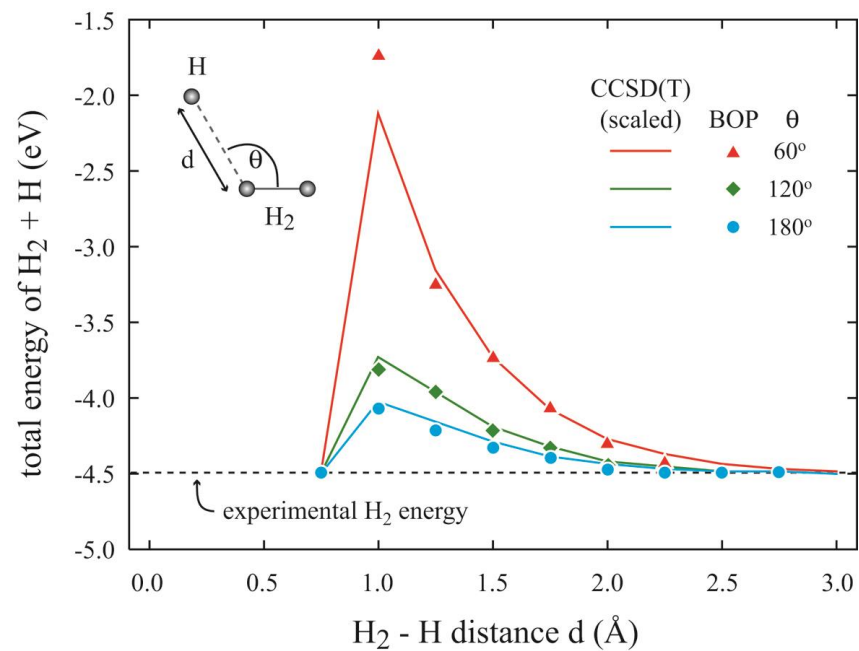
ADP	1.09
EAM-CY	-0.06
BOP	0.14
DFT	0.40
Exp.	0.45

# $H_2 + H \rightarrow H + H_2$ chemical reaction

Hydrogen crystal to  $H_2$  gas



$H_2 + H \rightarrow H + H_2$  energy profiles

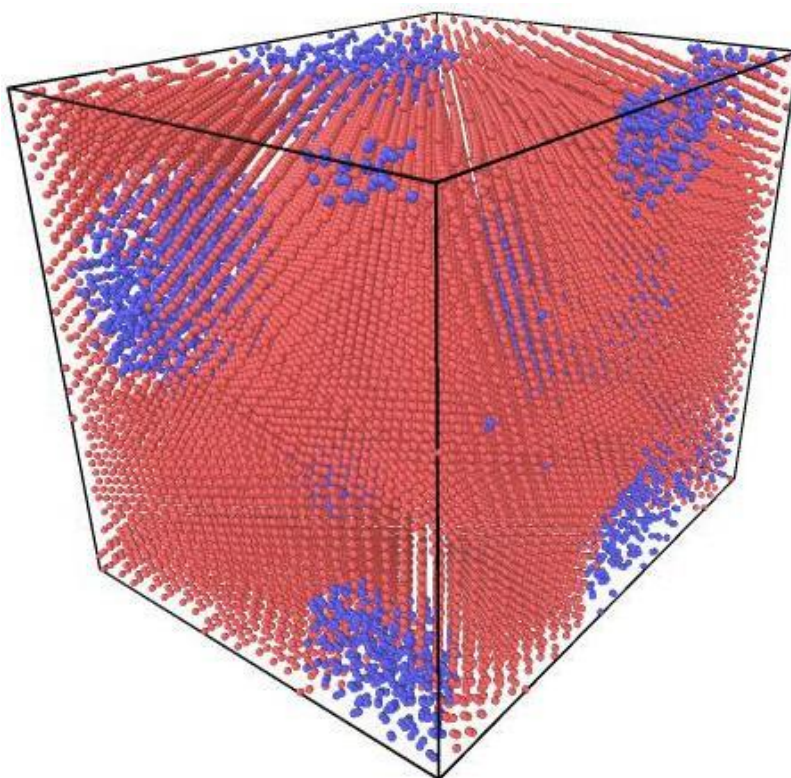


Our BOP captured the  $H_2 + H \rightarrow H + H_2$  reaction

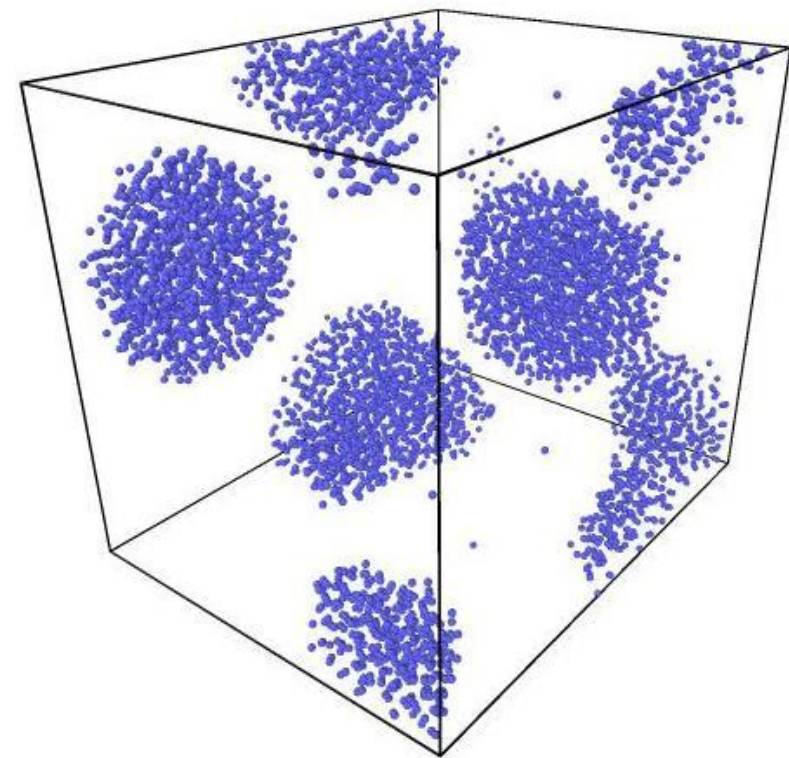


# Al + H<sub>2</sub> and Cu + H<sub>2</sub> Phase Separation

(a) N<sub>H</sub>/N<sub>Cu</sub> = 0.20 with both Cu and H shown

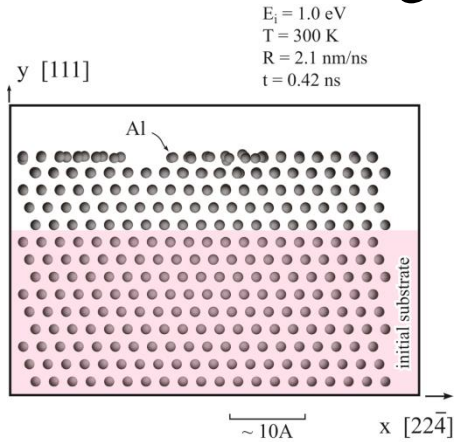


(b) Only H shown

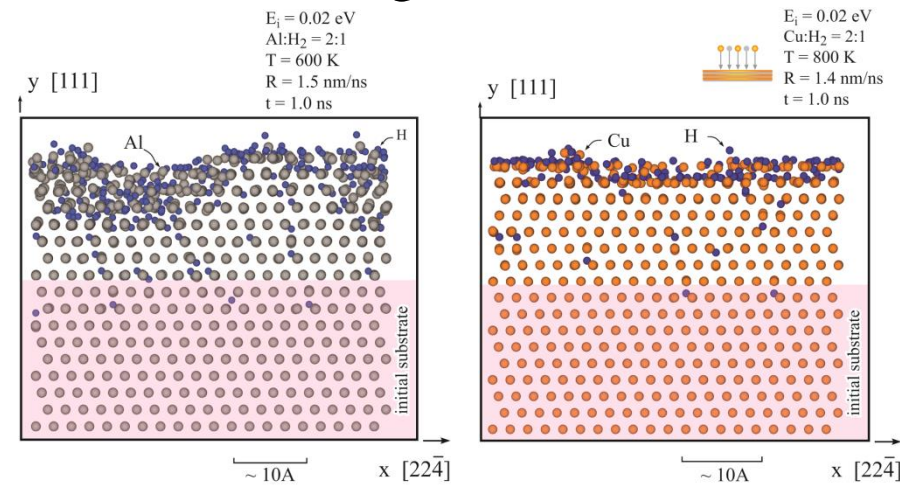


# MD growth simulations

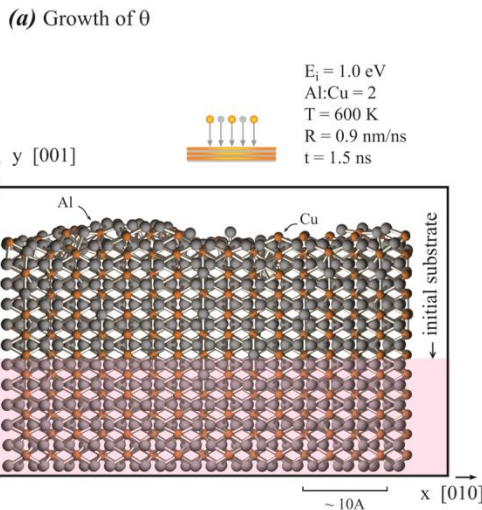
## Al and Cu growth without H



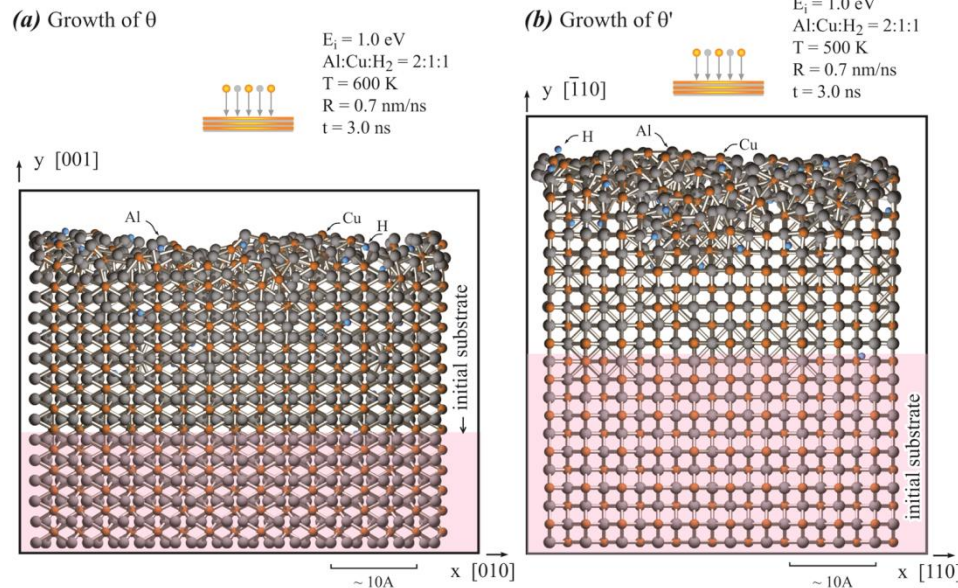
## Al and Cu growth with H



## $\text{Al}_2\text{Cu}$ ( $\theta$ and $\theta'$ ) growth without H



## $\text{Al}_2\text{Cu}$ ( $\theta$ and $\theta'$ ) growth with H



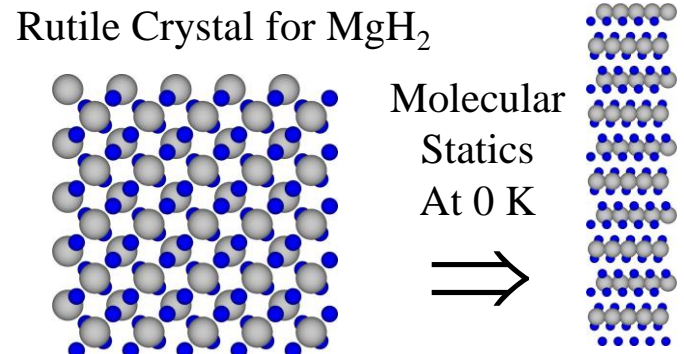


# Current status of our Mg-H analytical bond order potential

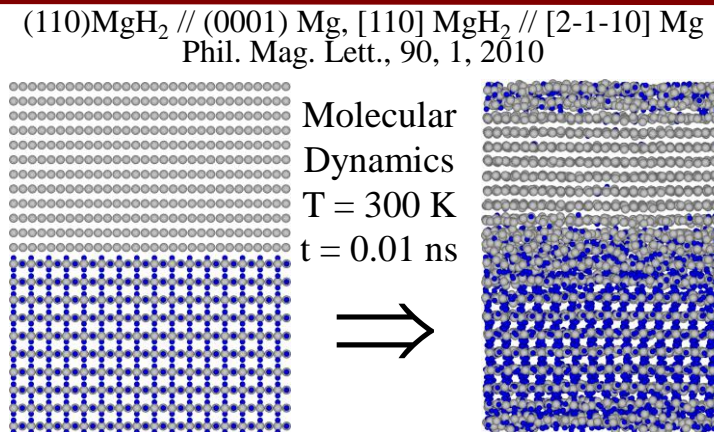
.....

# Issues of literature potentials

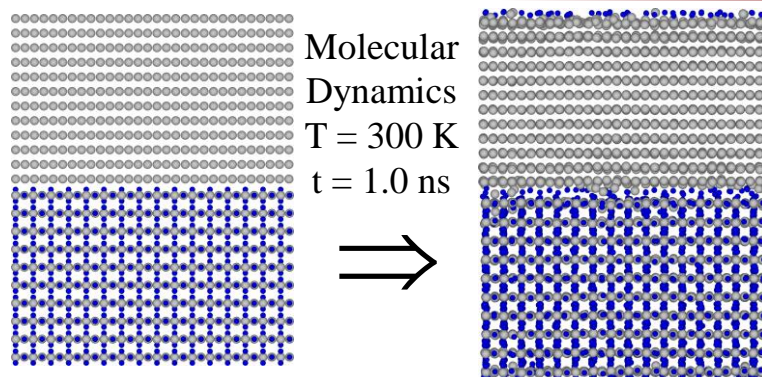
1. Literature Mg-H **EAM** potential developed by Ruda et al (ANALES DE LA ASOCIACION QUIMICA ARGENTINA, 84, 393, 1996) cannot maintain the correct  $\text{MgH}_2$  crystal structure even during 0 K;



2. Literature Mg-H **ReaxFF** potential developed by Cheung et al (S. Cheung, W. Q. Deng, A. C. T. van Duin, W. A. Goddard, J. Phys. Chem., 109, 851 2005) cannot maintain the correct  $\text{MgH}_2$  crystal structure during 300 K molecular dynamics (MD) simulations;

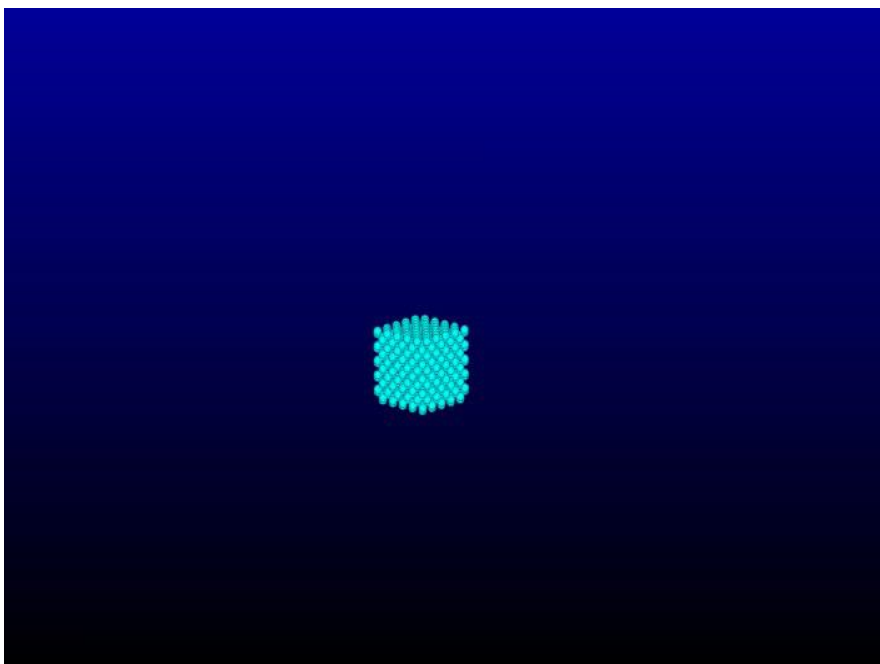


3. Our preliminary Mg-H **bond order potential** enables MD simulations of  $\text{MgH}_2$  crystals.

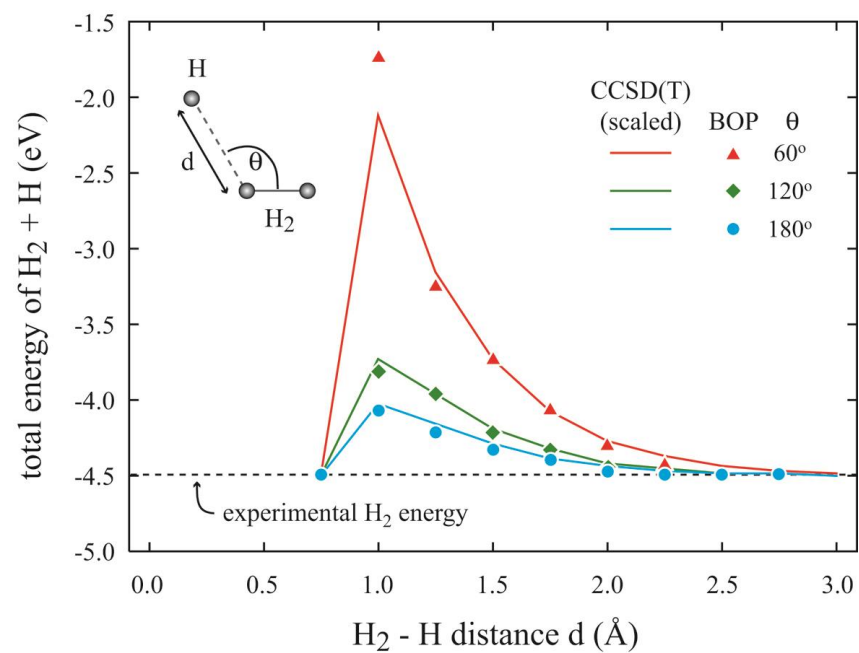


# $H_2 + H \rightarrow H + H_2$ chemical reaction

Hydrogen crystal to  $H_2$  gas



$H_2 + H \rightarrow H + H_2$  energy profiles

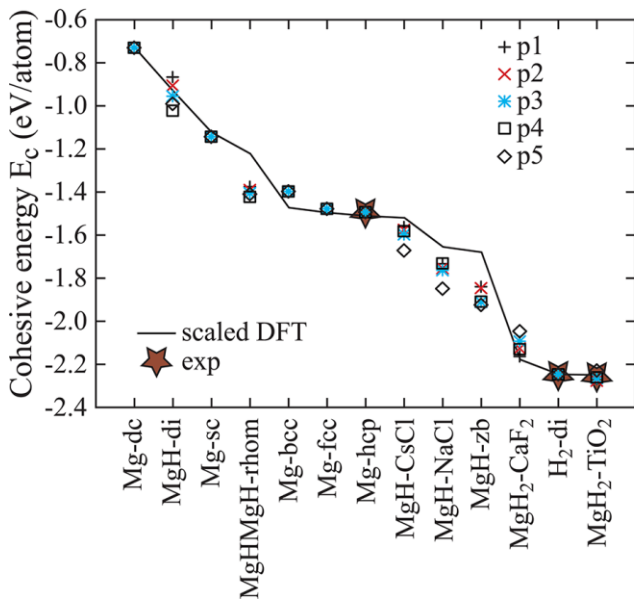


Our BOP captured the  $H_2 + H \rightarrow H + H_2$  reaction

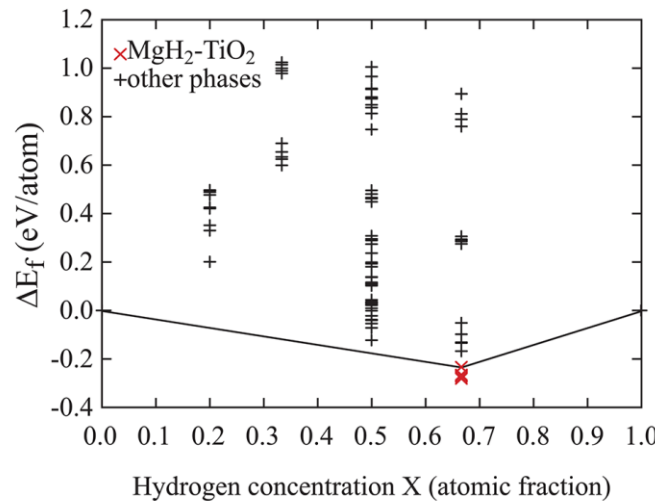
# Transferability

## Energy trends

(a) Cohesive energy  $E_c$



(b) Heat of formation  $\Delta E_f$  from all potentials

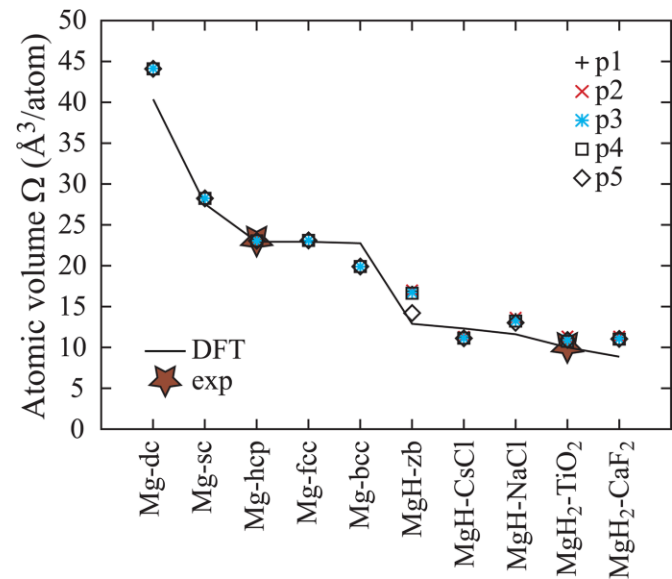


## Elastic constants of Mg-hcp

Table I. Elastic constants  $C_{11}$ ,  $C_{33}$ ,  $C_{44}$ ,  $C_{13}$ , and bulk modulus  $B = (2C_{11} + 2C_{12} + C_{33} + 4C_{13})/9$  in unit eV/Å<sup>3</sup>.

$C_{11}$		$C_{33}$		$C_{44}$		$C_{13}$		$B$	
Cal.	Exp.	Cal.	Exp.	Cal.	Exp.	Cal.	Exp.	Cal.	Exp.
0.40	0.40	0.42	0.41	0.11	0.12	0.14	0.14	0.23	0.23

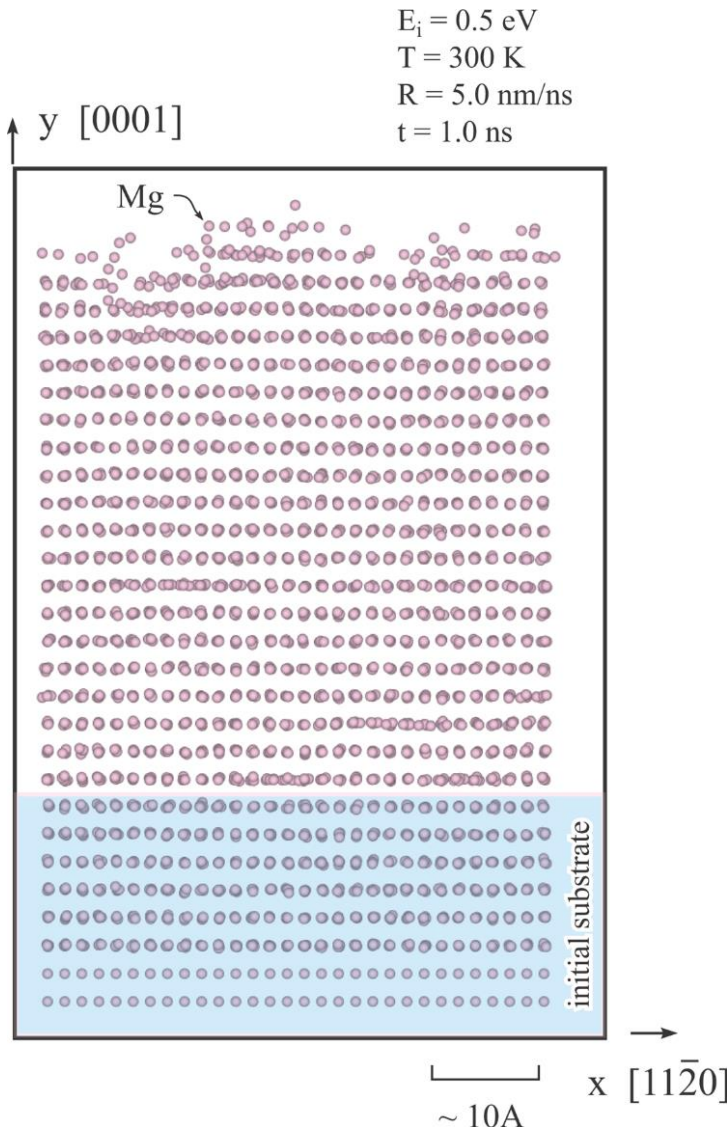
## Volume trends



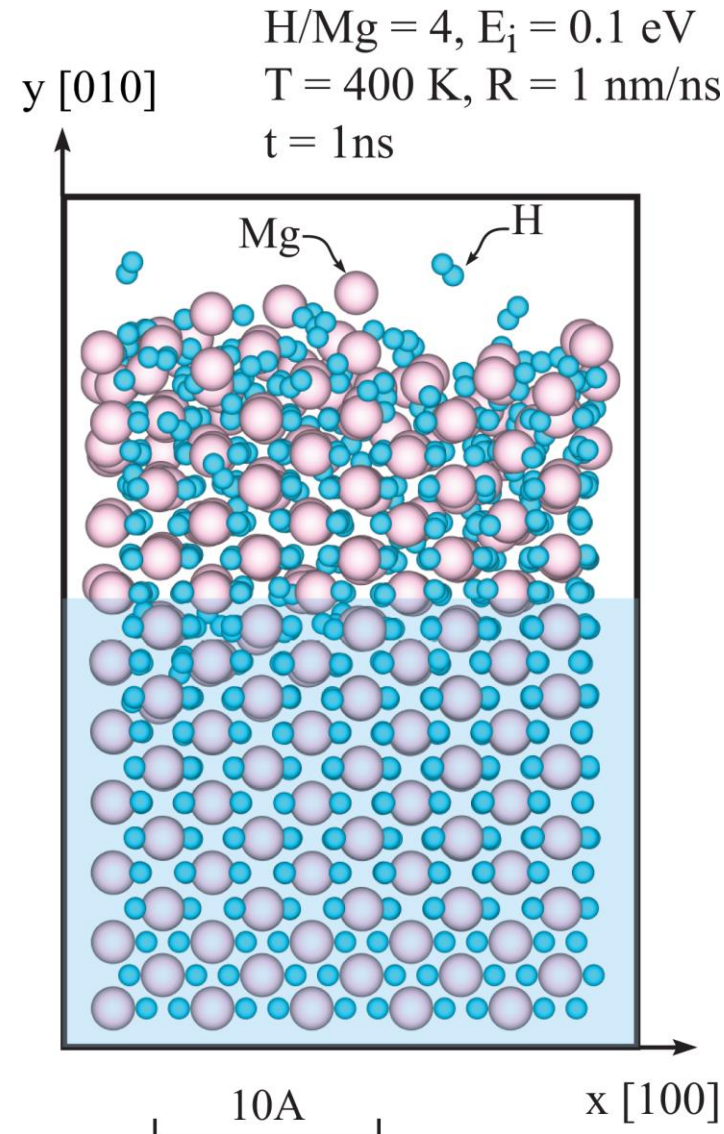


# MD Growth Simulations

## Crystalline growth of Mg-hcp

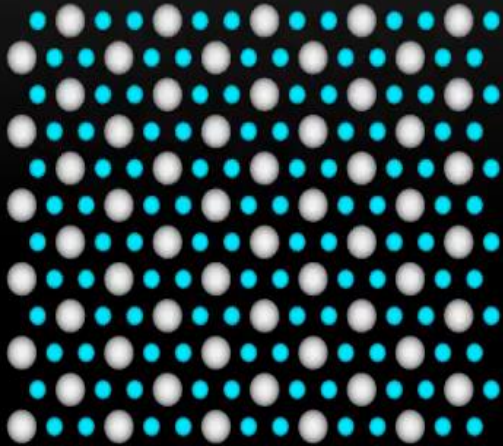


## Crystalline growth of MgH<sub>2</sub>-rutile





# Time-evolution of growth



# Summary

1. Our Fe-Ni-Cr EAM captures the four criteria critical for simulations of stainless-steels. Hydrogen is yet to be added;
2. Our Al-Cu-H BOP captures the high Al stacking fault energy, the stability of  $\text{Al}_2\text{Cu}$  compound, and the  $\text{H}_2/\text{H}$  chemical reaction;
3. Our Mg-H BOP captures the crystalline growth of the rutile phase of  $\text{MgH}_2$  hydride.